The generation of diesel exhaust particle aerosols from a bulk source in an aerodynamic size range similar to atmospheric particles

Daniel J Cooney[1]
Anthony J Hickey[2]

[1]Department of Biomedical Engineering; [2]School of Pharmacy, University of North Carolina, Chapel Hill, NC, USA

Abstract: The influence of diesel exhaust particles (DEP) on the lungs and heart is currently a topic of great interest in inhalation toxicology. Epidemiological data and animal studies have implicated airborne particulate matter and DEP in increased morbidity and mortality due to a number of cardiopulmonary diseases including asthma, chronic obstructive pulmonary disorder, and lung cancer. The pathogeneses of these diseases are being studied using animal models and cell culture techniques. Real-time exposures to freshly combusted diesel fuel are complex and require significant infrastructure including engine operations, dilution air, and monitoring and control of gases. A method of generating DEP aerosols from a bulk source in an aerodynamic size range similar to atmospheric DEP would be a desirable and useful alternative. Metered dose inhaler technology was adopted to generate aerosols from suspensions of DEP in the propellant hydrofluoroalkane 134a. Inertial impaction data indicated that the particle size distributions of the generated aerosols were trimodal, with count median aerodynamic diameters less than 100 nm. Scanning electron microscopy of deposited particles showed tightly aggregated particles, as would be expected from an evaporative process. Chemical analysis indicated that there were no major changes in the mass proportion of 2 specific aromatic hydrocarbons (benzo[a]pyrene and benzo[k]fluoranthene) in the particles resulting from the aerosolization process.

Keywords: diesel exhaust particles, aerosol, inhalation toxicology

Introduction

Chronic and acute exposure to airborne particulate matter (PM) and diesel exhaust particles (DEP) have been identified as human health hazards. Cohort epidemiologic studies have indicated that chronic exposure to PM is a likely risk factor in the formation of lung cancer as well as a potential noncancerous respiratory hazard (Pope et al 2002). Time series studies have shown that short term increases in levels of PM are associated with increased mortality and morbidity (Bell et al 2004). DEP are a likely contributor to the acute and chronic toxicity of inhaled PM and are a major component of ambient PM. DEP makes up approximately 6% of nationwide ambient $PM_{2.5}$ mass and considerably more in some urban areas (USEPA 2002). The extent of the DEP contribution to PM toxicity is not known because it is difficult to isolate the effects of exposure to diesel exhaust (DE) or DEP in humans. Some epidemiology studies involving groups of individuals exposed to elevated levels of DEP in the workplace have shown increases in relative risks of lung cancer and respiratory disease (Bhatia et al 1998; Lipsett and Campleman 1999; Sauvain et al 2003). Some indication of decreased pulmonary function (Gamble et al 1987) and increased mortality from cardiovascular disease (Edling and Axelson 1984) has also been noted in chronically exposed workers. A few studies have shown that short term pulmonary exposure to

Correspondence: Daniel J Cooney
Nektar Therapeutics, 201 Industrial Rd., San Carlos, CA 94070, USA
Email cooneyinsf@gmail.com

DE or DEP elicits an inflammatory response, marked by an increase in neutrophils and/or interleukin-8 (IL-8) in bronchoalveolar lavage fluid, in healthy volunteers (Rudell et al 1999; Salvi et al 1999; Salvi et al 2000). The majority of evidence for DEP-specific toxicity, however, comes from animal experimentation.

Animal experiments allow the study of effects of DEP exposure, which, with *in vitro* toxicology, elucidates the pathogenesis of disease following exposure. Chronic DE and DEP exposure affects laboratory animals by changing survival, pulmonary function, inflammation, histopathology, and cancer rates (Vinegar et al 1981; Lewis et al 1986; Iwai et al 1986; Henderson et al 1988; Nikula et al 1995). Pulmonary inflammation following acute exposure in animals has been repeatedly observed (Yang et al 1999; Nemmar et al 2003; Harrod et al 2003). A large number of *in vitro* studies have been conducted using various cells types to determine the cellular response to exposure to DEP and their components (Bayram et al 1998; Hiura et al 1999; Takizawa et al 1999, 2003; Don Porto Carero et al 2001; Li et al 2002; Amakawa et al 2003; Auferhide et al 2003; Baulig et al 2003). There are many questions and concerns, however, when drawing conclusions about the toxicity of a material in humans from exposure studies conducted in animals or cells. These concerns are amplified for a heterogeneous, inhaled toxicant, such as DEP, because of the complicated interaction between particle properties, deposition, and toxicity. The methods currently employed of assessing pulmonary toxicity of DEP in animals or cells in culture may not be representative of particles inhaled by humans.

DEP are often delivered to the lungs of animals as aqueous liquid instillations and the prevalent methodology for exposing cells is to spike an aqueous suspension of DEP at the apical surface of cells. Delivery of particles in aqueous suspension alters the particles themselves and the manner in which they are presented to the cells of the lung. These methods may be acceptable to identify certain potential mechanisms for DEP toxicity in the lung, but do not address issues specific to atmospheric DEP such as particle size and the interaction between insoluble and soluble compounds.

The deposition of particles in the lung is highly dependant on the properties of the particles. Particle size, specifically aerodynamic diameter, is of primary importance in the determination of probability and location of deposition of a particle in the lungs. DEP exist in the atmosphere in a trimodal size distribution with aerodynamic diameters ranging from 10 nm to more than 1 μm (Kittelson 1998). This size distribution makes them easily respirable and likely to deposit throughout the lungs (ICRP 1994). The nuclei mode (5–50 nm), containing droplets of organic and sulfur compounds and, potentially, solid carbon and metal particles, comprises a small fraction of the DEP mass, but the numerical majority of particles. The accumulation mode (100–1000 nm), consisting of aggregates of solid carbon particles with a number of adsorbed organic compounds, salts, and trace elements on the surface, makes up the majority of DEP mass. The coarse mode, comprised of larger aggregates (1–10 μm), is generally not significant in terms of number or mass. This size distribution needs to be reproduced in the lab in order to obtain realistic lung deposition patterns.

The organic compounds, averaging 20% to 40% of total mass for most DEP (USEPA 2002), are thought to be primarily responsible for the cancer and noncancer toxicity of DEP. The hundreds of compounds adsorbed to the surface of the solid carbon particles include at least 15 polyaromatic hydrocarbons (PAHs) or nitro-polyaromatic hydrocarbons (N-PAHs) that are considered to be potential or probable carcinogens by the US National Toxicology Program (Sauvain et al 2003). Their metabolism causes production of reactive oxygen species (ROS), which can be directly toxic by damaging lipids, proteins, and DNA, and can elicit an inflammatory response. All of these mechanisms require interaction with the particles and are therefore dependent on the surface properties of those particles, which may be altered by suspension in liquid.

The limitations of employing DEP suspensions have been identified and a number of systems to expose animals and cultured cells to freshly generated DE and DEP have been developed (Massey et al 1998; Wolz et al 2002). These methods represent a realistic deposition scenario, but have several major drawbacks. The systems employed require considerable space, money, and time to set up, operate, and maintain. Freshly generated DEP may not represent atmospheric DEP because effects of aging are not taken into account. Due to the complexity of the combustion process, engine-based exposure systems inevitably lead to inter-laboratory variability in the particles produced. Regeneration of DEP aerosols from small quantities of bulk powder in particle sizes relevant to atmospheric pollution for laboratory testing is a desirable technique to develop. A low dose delivery approach would allow deposition of particles in a realistic size range, and aerosols with the same properties could be generated in multiple locations following distribution of samples from a single bulk source.

When collected by filtration and stored in a sealed vessel, DEP are forced into close contact with each other, promoting

aggregation. The production of aerosols with a small average particle diameter from an aggregated powder is not easily accomplished. Some devices, including the Wright dust feeder and fluidized bed generators, generate aerosols from a bulk source of powder (Hinds 1999). These devices require relatively large volumes of bulk powder and are not design for generating single small doses of aerosol. The creation of aerosols with small particle sizes from small quantities of powder has been an aim of the pharmaceutical industry for years. Metered dose inhalers (MDIs) are used in the pharmaceutical industry to deliver aerosols by inhalation (Atkins and Crowder 2004). Suspension MDIs allow de-aggregation of a powder in an inert liquid propellant. Following aerosolization, the propellant evaporates, leaving only the suspended particles. The size of the resultant particles can be modulated by controlling the suspension concentration, initial droplet size, and level of de-aggregation in the suspension.

This study provides a characterization of DEP aerosols generated in small doses from a bulk source using the principals of metered dose inhaler technology. The mass and number-based aerodynamic particle size distributions of the aerosols were determined by cascade impaction, the physical size and morphology of deposited particles were examined by scanning electron microscopy (SEM), and a preliminary chemical analysis comparing pre- and post-aerosolized DEP is presented.

Materials and methods

Sources of diesel exhaust particles

DEP were generated at the EPA main campus in Research Triangle Park, North Carolina using a 30 kW (40 hp) 4-cylinder Deutz BF4M1008 diesel engine connected to a 22.3 kW Saylor Bell air compressor to provide a load. The engine and compressor were operated at steady-state to produce 0.8 m^3/min of compressed air at 400 kPa. This translates to approximately 20% of the engine's full-load rating. Emissions from the engine were diluted with filtered air (3:1) to near ambient temperatures (~35 °C) and directed to a small baghouse (Dustex Model T6-3.5-9 150 ACFM pyramidal baghouse using nine polyester felt bags). Gram quantities of DEP were collected using reverse air pulsing. Once collected, the DEP samples were stored in sealed glass containers in a refrigerator (~4 °C).

DEP quantification

For the preparation of turbidity concentration curves, DEP were suspended in ethanol, placed in an ultrasonic bath (FS21H; Fisher Scientific, Pittsburgh, PA, USA) for 30 s, serially diluted, and sonicated again briefly before reading light extinction at 700 nm (EXT_{700}) (UV160U spectrophotometer; Shimadzu). To determine the effect of sonication time on EXT_{700}, suspensions of DEP in ethanol (7.95 μg/ml) were placed in a sonication water bath (Model 2510; Branson, Danbury, CT, USA) for 30, 60, or 180 seconds with swirling every 15 seconds. The suspensions were removed from the bath, swirled, and EXT_{700} was measured (Libra S22; Biochrom, Cambridge, UK).

Suspension preparation

DEP was added to plastic-coated clear glass bottles (Wheaton Science Products, Millville, NJ, USA) fitted with 25 μl metering valves (Bespak, Apex, NC, USA) that were sealed by crimping (Aero-Tech Laboratory Equipment Company, Worcester, NY, USA). Prior to fitting, holes that connected the valve stem to the bottle during actuation were drilled in some of the metering valves, creating nonmetered, continuous valves. The bottles were then filled with 20 g of HFA134a (hydrofluoroalkane 134a) through the valve using a pressure burette (Aero-Tech) at 175 PSI. The resultant suspensions (0.2, 1.0, and 5.0 mg DEP/g HFA134a) were placed in an ultrasonic bath for 10 minutes to disperse the particles. All aerosols were generated using an actuator with a 300 μm diameter round orifice.

Suspension stability

Stability of 0.2, 1.0, and 5.0 mg/g suspensions was estimated by observing aggregation and sedimentation of the suspended particles as functions of time following 10 seconds of vigorous vortex mixing (Vortex Genie 2; Fisher Scientific). The general appearance of the suspension (opacity, formation of large aggregates, and/or sedimentation) was monitored in the first 5 minutes following mixing. If the particles sedimented as a single, aggregated mass, the time it took for the top of the aggregate to sediment to specific heights (5 mm apart) was recorded (n = 3 for each of 3 bottles for each concentration). The relative concentrations of suspended DEP were estimated by measuring EXT_{700} (UV160U) through the glass bottles from 5 to 80 minutes following mixing (n = 3 for each of 3 bottles for each concentration). For EXT_{700} measurements, the bottles were centered between the light source and detector of the spectrophotometer. Suspensions were also observed 24 hours after mixing.

Emitted dose

The emitted doses for 0.2, 1.0, and 5.0 mg/g suspensions in bottles fitted with 25 μl metered valves and for a 1.0 mg/g

suspension fitted with a continuous valve were determined by actuation into an emitted dose device (EDD; MSP Corporation, Shoreview, MN, USA) fitted with a 0.1 μm polycarbonate filter (Millipore) operated at 30 L/min. The suspensions were vortexed for 10 seconds prior to testing and a separate actuator was used to prime the suspensions 3 times. Because of the limit of detection of the EXT_{700} method, 10, 5, and 5 actuations were used for each run for 0.2, 1.0, and 5.0 mg/g suspensions, respectively (n = 6 per concentration). One actuation of approximately 1 second was used for the 1.0 mg/g suspension with the continuous valve (n = 5). A pause of at least 5 seconds between actuations allowed the bottles to be swirled vigorously by hand to minimize aggregation and settling. DEP were recovered by washing the device, filter, and actuator in ethanol in an ultrasonic bath (Vortex Genie 2, Fisher Scientific) and were quantified. The mass of each bottle was recorded before and after each experiment to facilitate calculation of the amount of propellant used. Expected DEP deposition was calculated by multiplying the amount of propellant used by the DEP concentration.

Size characterization

Deposition of DEP aerosols as a function of aerodynamic diameter was measured using a nonviable cascade impactor (NVCI, ThermoAndersen, Smyrna, GA, USA) and an electrical low pressure impactor (ELPI; Dekati, Finland). The NVCI was operated at a flow of 28.3 l/min with a United States Pharmacopeia (USP) sampling inlet. Deposition was quantified by washing the actuator, inlet, and stages in ethanol followed by quantification. 20, 10, and 5 actuations (0.2, 1.0, and 5.0 mg/g) were used for each run with metered valves and 5 actuations were used for each run with a continuous valve due to the limit of detection of the quantification method (n = 3 per concentration). The suspensions were primed 3 times with a separate actuator prior to testing, allowing at least 5 seconds between actuations. Bottles were swirled vigorously by hand between actuations to prevent aggregation and settling. To examine the effect of evaporation time on deposition, the same experiments were repeated for bottles with metered valves with a 78 cm long, 5 cm diameter tube serving as a spacer. The volume of the spacer was approximately 1.5 L, which allowed approximately 3 seconds of added travel time for the aerosol from actuator to inlet.

The ELPI was operated at 30 L/min flow rate with sintered metal collection stages and the filter stage in place. The aerosol was introduced to the inlet with and without the spacer described above and data was gathered by averaging deposition from 5 sequential actuations with swirling in between (n = 3 per concentration).

Chemical composition

A method for determining the concentration of benzo[a]pyrene (B[a]P) and benzo[k]fluoranthene (B[k]F) was used to determine the effect of suspension in HFA134a on the compounds adsorbed to the surface of the DEP. The method was adapted from a dual wavelength fluorometric detection method (Masaki et al 2005). Fluorescence concentration curves for B[a]P and B[k]F dissolved in dichloromethane (DCM, 0–500 ng/mL) were made by serial dilution (n = 2 per compound). The fluorescence of each concentration of each compound was read at an emission wavelength of 429 nm with excitation wavelengths of 370 and 395 nm with 5 nm slits (LS50B luminescence spectrometer, PerkinElmer). The equations for fluorescence as function of concentration at each excitation wavelength were combined (total fluorescence = fluorescence from B[a]P + fluorescence from B[k]F), yielding two equations. These equations were solved for the unknowns of B[a]P and B[k]F concentrations.

Bulk DEP2 was suspended in DCM in glass vials at concentrations of 0.25 to 2.5 mg/ml to determine the concentration of the compounds adsorbed onto DEP (n = 6). DEP2 suspended in HFA134a (1.0 mg/g) and aged 6 months at room temperature or aged less than 1 week at 4 °C (fresh) was aerosolized and deposited onto the filter of an EDD (n = 3 per condition). The filter was added to a glass vial and suspended in DCM (0.1–0.5 mg/mL DEP). All bulk DEP and DEP aerosol suspensions were placed in an ultrasonic bath for 30 minutes to dissolve surface adsorbed compounds. The suspensions were then centrifuged at 10,000 g for 15 minutes to pellet the suspended particles. Five ml of the supernatant were added to a new glass vial and allowed to evaporate at room temperature. Solutions of B[a]P and B[k]F in DCM (0–500 ng/mL) were made by serial dilution for determine the collection efficiency of the evaporation and extraction methods. Five ml of each concentration of each compound were added to glass vials and allowed to evaporate.

The remaining solids from the bulk and aerosol DEP and known PAH concentrations were dissolved in 5 ml of methanol. The methanol solutions were cleaned with a solid phase extraction column (1cc HLB, Waters). For extraction, the columns were conditioned with 1 mL DCM and rinsed with 1 mL methanol then 1 mL water. After 3 ml of sample was added, columns were rinsed with 1 ml of water and the compounds were eluted with DCM. The fluorescence was

read at an emission wavelength of 429 nm with excitation wavelengths of 370 and 395 nm, as described above.

Morphology

Small amounts of DEP from the bulk container were placed on 13 mm diameter round glass cover slips and were examined by SEM (JEOL JSM-6300, JEOL America, Peabody, MA, USA). Cover slips were sputter-coated with gold-palladium for 60 seconds prior to imaging to improve conductivity (Model E-5200, Electron Beam Services, Agawan, MA, USA). Aerosols from a 1.0 mg/g DEP suspension were deposited on glass cover slips placed on all stages of the NVCI operated at 60 l/min and aerosols from 0.2, 1.0, and 5.0 mg/g DEP suspensions were deposited on glass cover slips placed on stages 1, 2, and 3 of the ELPI. These cover slips were sputter coated and imaged by SEM as described above.

Results and discussion

Quantification

The turbidity concentration curves were linear over the range of 0–60 μg DEP/ml ethanol, with values of the square of correlation coefficient for linear regression (R^2) > 0.99. The EXT_{700} values of the 7.95 μg/ml DEP suspension following sonication for 30, 60, and 180 seconds were 0.141 ± 0.001, 0.141 ± 0.001, and 0.144 ± 0.004, respectively. These values were not dependant on time after sonication when monitored up to 15 minutes (results not shown). This indicated that it was acceptable to sonicate for as little as 30 seconds and to wait up to 15 minutes following sonication to measure light extinction.

Suspension stability

The rates of aggregation and sedimentation were very different for the range of suspension concentrations. The 0.2 and 1.0 mg/g suspensions underwent cluster deposition, but at different rates. The lowest concentration (0.2 mg/g) showed the smallest extent of visual aggregation. Mixing produced uniform, slightly translucent, suspensions. The suspensions remained uniform, without individually distinguishable aggregates, for the first 5 minutes. Some large flocculates were seen by 10 seconds after mixing in the 1.0 mg/g suspensions. The majority of these large flocculates settled to the bottom of the bottle by 1 minute after mixing, leaving the remaining suspension more translucent than the 0.2 mg/g suspensions. The 5.0 mg/g suspensions underwent collective settling. A flocculate formed in the entire volume of each bottle within seconds after mixing. The flocculate height dropped linearly from the top of the propellant level for approximately 1 minute, after which the height dropped very slowly. The velocity of sedimentation was calculated as 0.71 mm/sec by fitting a line to the data up to 45 seconds (4 data points, $R^2 = 0.94$). The propellant above the gelled mass in the 5.0 mg/g suspension appeared transparent with few, if any, suspended particles.

The average EXT_{700} values for the 0.2 and 1.0 mg/ml suspensions decreased linearly as a function of the log of time from 5 to 80 minutes ($R^2 > 0.99$). The EXT_{700} values for the 5.0 mg/g suspension did not change significantly over this time period because most particles had sedimented with the flocculate previously. A concentration curve for DEP in HFA134a could not be produced, but light extinction of particles in suspension is directly proportional to concentration, provided the particles are of the same size (Gebhart 2001). This proportionality indicates that the concentration of particles in suspension decreased linearly as a function of the log of time following an initial lag time. The rate of decrease was greater for the 0.2 mg/g suspension because the volume concentration after 5 minutes, and thus the aggregation rate and sedimentation rate, was greater. The rates of aggregation and sedimentation were much greater in the first few minutes for the 1.0 mg/g suspension, but once the large flocs had formed a sediment, the volume of remaining suspended particles was less than 0.2 mg/g. The slopes and intercepts of linear regressions were recorded for each run of each bottle and there were no statistically significant differences between bottles or runs (all $p > 0.05$, ANOVA).

Twenty-four hours after mixing, DEP were not detected in suspension. The propellant was transparent, but did vary slightly in color with DEP concentration. The propellant from 0.2 mg/g suspension did not appear different in color to propellant without DEP. The propellant from the 1.0 mg/g had a slight yellowish tint and that tint was darker in the propellant from the 5.0 mg/g suspension, indicating dissolution of adsorbed compounds in the propellant.

It was clear that when left unstirred, DEP aggregate in suspension in HFA134a in concentrations of 0.2 to 5.0 mg/g. The rate of this aggregation and the sedimentation of those aggregates was dependant on initial concentration. It was also clear that the particles de-aggregate reproducibly when the same energy was added to the suspension in the form of mixing. The aggregation, settling, and concentration as a function of time were reproducible upon mixing. Caking did not occur in suspensions left undisturbed up to 6 months. The degree of particle aggregation in the first seconds after mixing the suspensions is unknown and the use of these suspensions to

create reproducible aerosols requires actuation very soon after mixing, but should by reproducible if that time is kept short and constant. It was also clear from the color of the liquid following complete settling that there are compounds present on the DEP that dissolved in the propellant to some extent. The exact compounds that dissolve and the extent to which they dissolve are unknown, but it should be noted that some dissolution of the adsorbed compounds does occur in HFA134a.

Emitted dose

The volume of suspension emitted per actuation and the expected DEP deposition calculated from that volume are shown in Table 1. The metering valves are reported to emit 25 μL per actuation, but the three valves used in these experiments delivered an average of 27.9 to 28.9 μL per actuation. Approximately 10 times (293 ± 19 μL) the suspension volume was delivered from each actuation of the continuous valve.

The mass of DEP recovered from the actuator, the EDD, the addition of those (total deposition), and the percent recovery (total/expected deposition × 100) are also shown in Table 1. Recovery ranged from 96.0% to 97.8 % and there are several possible reasons for recovery below 100%. DEP may have been incompletely washed from the emitted dose device, filter, or actuator because of the small volumes of ethanol used. It was also expected that a portion of the DEP mass flowed through the filter and was not captured because the filters used are designed to capture only particles larger than 100 nm. The data gathered from the ELPI (reported below) shows that a significant fraction of particles in the aerosols was smaller than 100 nm. However, the fraction of particles smaller than 100 nm was not likely to contain 2%–4% of the total mass. It is possible that a portion of the DEP mass was aggregated in the bottle to a size that was unable to pass into the metering chamber, but this was also unlikely because the 5.0 mg/g suspension, in which aggregation occurred the fastest, had the highest recovery.

Size characterization: NVCI

The total mass of DEP collected (actuator, inlet, and NVCI) per actuation and the mass of DEP collected on the stages of the NVCI per actuation are shown in Table 2. The recoveries of the aerosols from the 0.2, 1.0, and 5.0 mg/g suspensions fitted with metered valves were 85.1% ± 1.1%, 84.6% ± 5.3%, 93.7% ± 2.6%, respectively. The recovery of the aerosol from the 1.0 mg/g suspension fitted with a continuous valve and was 89.7% ± 2.1%. Recovery below 100% of nominal mass may be explained as with the emitted dose. The last stage of the NVCI has a cutoff diameter of 300 nm, allowing a fraction of small particles to pass though without depositing.

DEP deposition on each stage of the NVCI, the sampling inlet, and the actuator, as percentages of total expected dose for each suspension concentration is shown in Figure 1a. The deposition patterns in the NVCI were similar among the concentrations, with a slight increase in the deposited fraction in the middle size range (stages 3 and 4, 1.8–5.0 μm) and a decrease in deposited fraction in the smaller size range (stages 6 and 7, 0.3–1.0 μm) as suspension concentration increased. The proportion of particle mass deposited in the inlet was much greater for the 5.0 mg/g suspension than for the 0.2 or 1.0 mg/g suspensions. This may be explained by a higher proportion of large particles impacting in the back of the inlet for the 5.0 mg/g suspension.

Similar DEP deposition patterns in the NVCI were observed when the spacer was used (Figure 1b). There was a slight decrease in the mass deposited in the smaller stages for the 0.2 mg/g suspension and an increase in the deposition on most stages for the 5.0 mg/g suspension. When the deposition on each stage is normalized for the width of the particle

Table 1 Data and calculations from the emitted dose device (mean ± SD, n = 6)

Product Information	25 μL Metered valve			Continuous valve
	0.2 mg/g	1.0 mg/g	5.0 mg/g	1.0 mg/g
Actuations per run	10	5	5	1
Suspension/actuation (μL)	27.9 ± 0.2	28.9 ± 0.2	28.2 ± 0.1	293 ± 19
Expected diesel exhaust particles dose (μg)	67.5	175	853	354 ± 23
Actuator deposition (μg)	18 ± 1	43 ± 2	186 ± 1	102 ± 11
Device deposition (μg)	47 ± 1	125 ± 5	648 ± 7	239 ± 18
Total deposition (μg)	65 ± 1	168 ± 6	834 ± 6	341 ± 23
Deposition per actuation	6.5 ± 0.1	33.6 ± 1.2	166.8 ± 1.2	341 ± 23
Percent recovery	96.3 ± 1.5	96.0 ± 3.4	97.8 ± 0.7	96.4 ± 1.3

Table 2 Total mass recovered, mass recovered from the stages of the nonviable cascade impactor (NVCI, n = 3), and number deposition on the stages of the electronic low pressure impactor (ELPI, n = 5) per actuation (mean ± SD)

Measured particle property	Spacer	Diesel exhaust particles concentration (mg/g)			
		0	0.2	1.0	5.0
Total mass/actuation (μg)	No	NA	5.7 ± 0.1	29.6 ± 1.9	159.7 ± 4.4
NVCI mass/actuation (μg)	No	NA	3.7 ± 0.1	19.2 ± 0.7	76.2 ± 3.7
NVCI mass/actuation (μg)	Yes	NA	3.1 ± 0.1	20.4 ± 1.2	90.1 ± 3.5
Number/actuation ($\times 10^8$)	No	19.3 ± 3.7	44.7 ± 8.6	58.4 ± 2.9	53.8 ± 7.6
Number/actuation ($\times 10^8$)	Yes	3.7 ± 0.4	20.9 ± 0.7	31.3 ± 0.8	30.3 ± 1.3

size range (in logarithms) collected on each stage, creating histograms similar to particle size distributions (Figure 2) these differences can be easily observed. The particle size distributions for each concentration were multimodal with primary maxima <2 μm (Mass Mode 1, MM1) and secondary maxima in the 5–6 μm range (Mass Mode 2, MM2). There were slight variations in the location of the maxima, which are discussed in conjunction with the ELPI data below. The location of these maxima better describe the distributions than estimation of mass median aerodynamic diameter. Calculations of geometric standard deviation could only be performed if the distributions were log-normal with a single

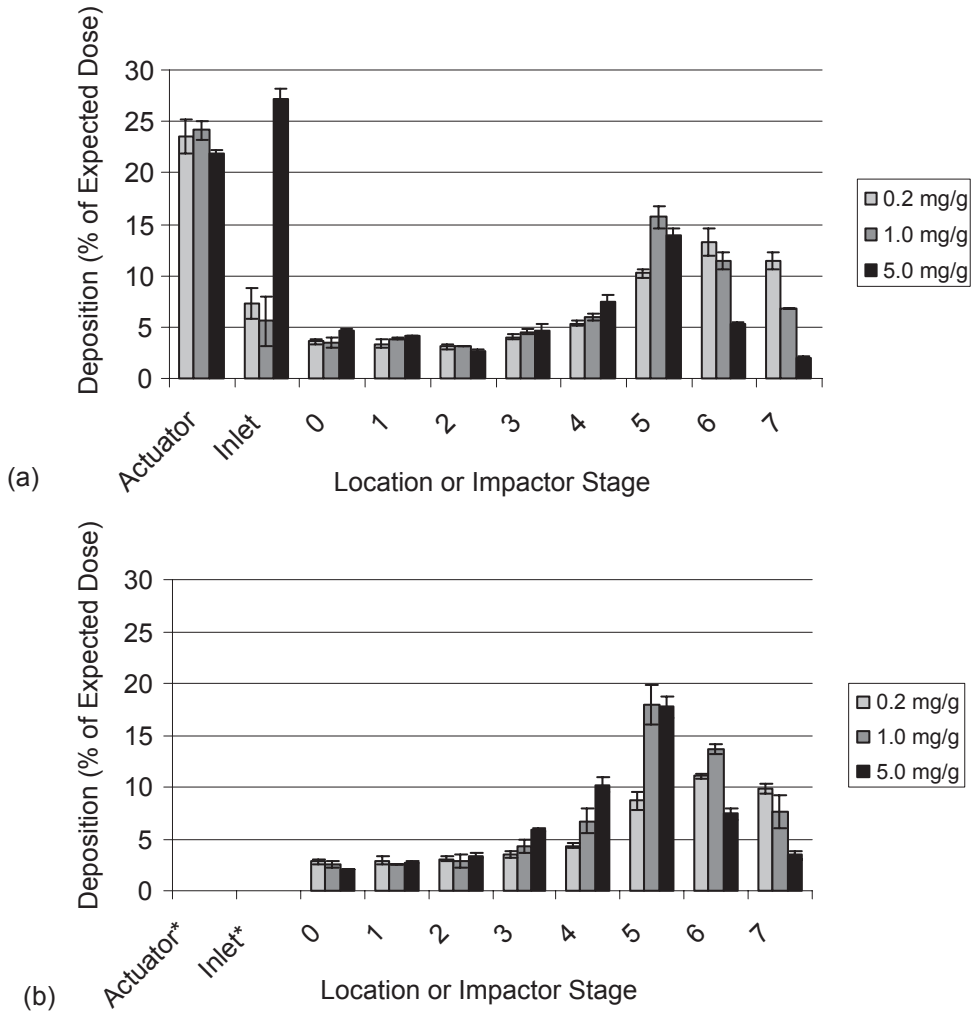

Figure 1 Percentage of expected total diesel exhaust particle dose deposited per actuation in actuator, sampling inlet, and nonviable cascade impactor (**a**) without and (**b**) with the spacer (mean ± SD, n = 3).
Note: *Actuator and inlet deposition were not calculated when the spacer was used.

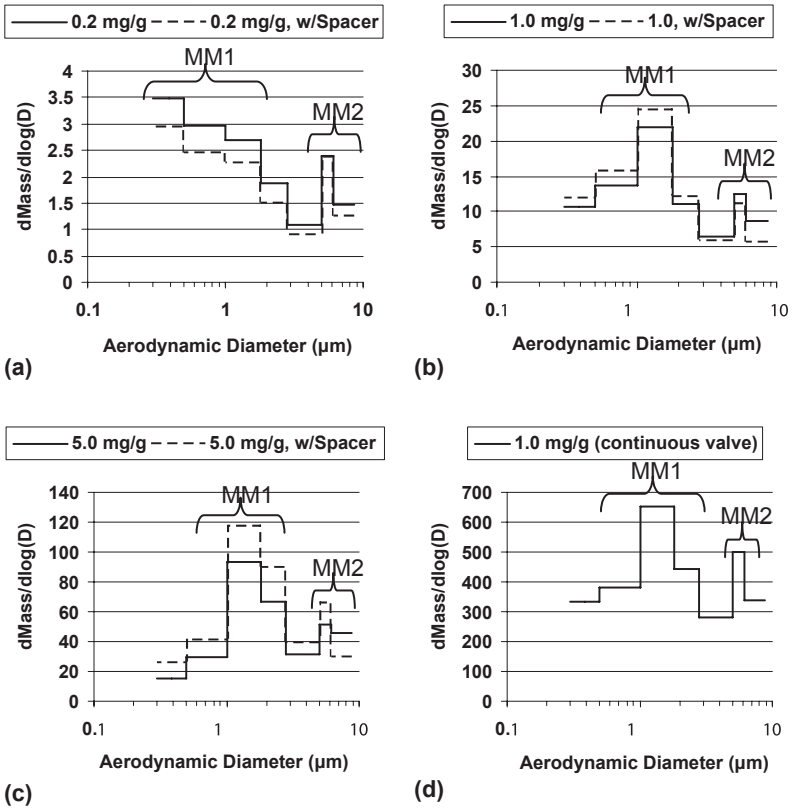

Figure 2 Particle size distributions by mass of diesel exhaust particle aerosols deposited in the nonviable cascade impactor with and without the spacer (mean, n = 3). Two apparent size modes, Mass Mode 1 (MM1) and Mass Mode 2 (MM2), are labeled.

mode. Since this was not the case, this calculation was not performed.

The particle size distribution of the aerosol from the 1.0 mg/g suspension with the continuous valve (Figure 2d) was similar to the distribution of the aerosol from the 1.0 mg/g suspension with the metered valve (Figure 2b). There was an increase (18.4 ± 3.4% compared to 5.6 ± 2.4%) in fractional inlet deposition for the continuous valve that may have been due to a change in plume shape resulting from a change in actuation duration.

Size characterization: ELPI

The total numbers of particles detected by the ELPI for each DEP suspension fitted with a metered valve are shown in Table 2. A statistically smaller number of particles deposited from the aerosol of the 0.2 mg/g suspension than from the other DEP aerosols with and without a spacer ($p < 0.05$, ANOVA). This decrease may be explained by a decrease in average particle size, as is discussed below, and an associated increase in number of particles small enough to pass through the filter and remain uncounted. The presence of droplets without DEP, also discussed below, may have also contributed to the decrease.

The total particle numbers for the aerosol from the propellant alone were much smaller than the other formulations, but were greater than zero. This indicates that the propellant had not completely evaporated by the time the aerosol reached the ELPI or that there was a contaminant, such as dissolved water, remaining. Water is somewhat soluble in HFA134a (Atkins and Crowder 2004) and could have remained after the propellant had evaporated.

The number of particles that deposited per actuation on each stage of the ELPI for each formulation with and without use of the spacer is shown in Figure 3. The pattern of deposition, like for mass deposition in the NVCI, is similar for all the formulations. For each formulation, the largest number of particles deposited on the filter stage (7–25 nm), with a general trend of decreasing particle deposition in the higher stages. The use of the spacer decreased the average number and standard deviation of particles counted per actuation on each stage for all formulations. These decreases in deposition may have been due to collection of particles in the spacer, particularly in the flow transition regions. Although if spacer deposition did occur, it was either limited to smaller particles that did not constitute much of the particle

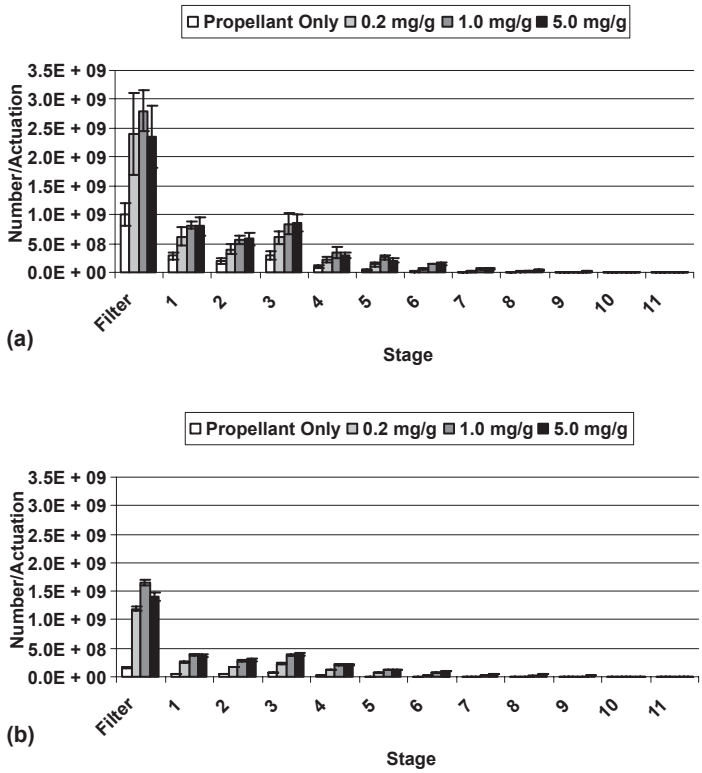

Figure 3 Number of particles deposited per actuation on each stage of the electronic low pressure impactor (**a**) without and (**b**) with the spacer (mean ± SD, n = 5).

mass (not seen in the NVCI data) or was confounded with the change in deposition in the inlet. The mass deposited in the NVCI was lower for 0.2 mg/g, approximately the same for 1.0 mg/g, and higher for 5.0 mg/g with the addition of the spacer. It was not easy to discern if the decreases in deposition in the ELPI were dependant on particle size because of the large standard deviations in the upper stages.

The decrease in number may also be explained by evaporation of propellant and/or other molecules. There was an approximately 50% decrease in deposition for the suspension formulations on each stage and an 80% decrease for the propellant only formulation. This difference cannot be explained with deposition in the spacer. If the aerosol from the propellant only formulation contained particles of water, some may have evaporated to a size smaller than was detectable by the ELPI.

The number deposition on each stage was normalized for the width of the particle size range (in logarithms) collected on each stage, creating histograms similar to particle size distributions (Figure 4). The number distributions of the suspension formulation were similar and appear to be multimodal with primary maxima <100 nm (Number Mode 1, NM1) and secondary maxima at approximately 300 nm (Number Mode 2, NM2). These distributions are discussed in conjunction with the mass distributions below.

Size characterization: Discussion

The mass and number-based particle size distributions appear to be bimodal, but when taken together indicate a probable trimodal aerosol particle size distribution. There were large numbers of nanoparicles (NM1) that would not be seen in the data from the NVCI because particles in this size range are too small to deposit in the device and contain very little mass. NM2 likely represents the same particle mode that is represented by MM1. The shift in location on the particle diameter axis from NM2 (~0.2–0.3 μm) to MM1 (0.5–1.5 μm) is typical of particle size distributions based on number and mass [mass ∝ (number × diameter^3)]. The number of particles contained in MM2 was likely too small for that mode to be seen in the ELPI data. The size distributions of suspension MDI aerosols are functions of the initial droplet sizes and the number of suspended particles and dissolved material that each droplet contains. If the aerosol particle size distribution was trimodal, the initial droplet distribution was likely trimodal. A diagram of the potential size distribution of droplets and final aerosol particles is shown in Figure 5. It has been shown

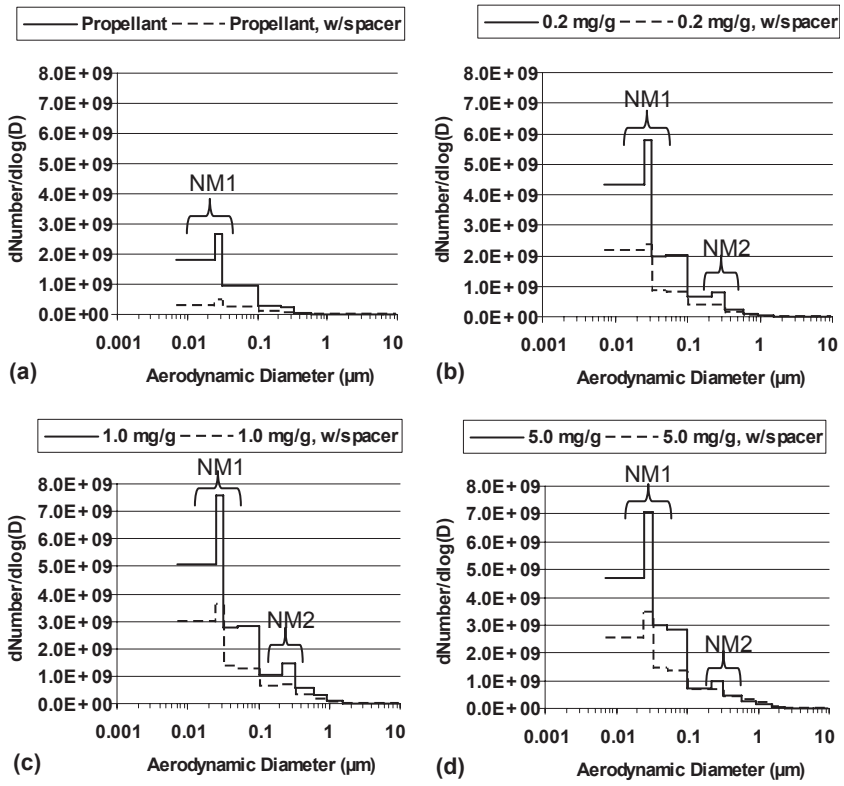

Figure 4 Particle number distributions of aerosols deposited in the electronic low pressure impactor with and without the spacer (mean, n = 5). Two apparent size modes, Number Mode 1 (NM1) and Number Mode 2 (NM2), are labeled.

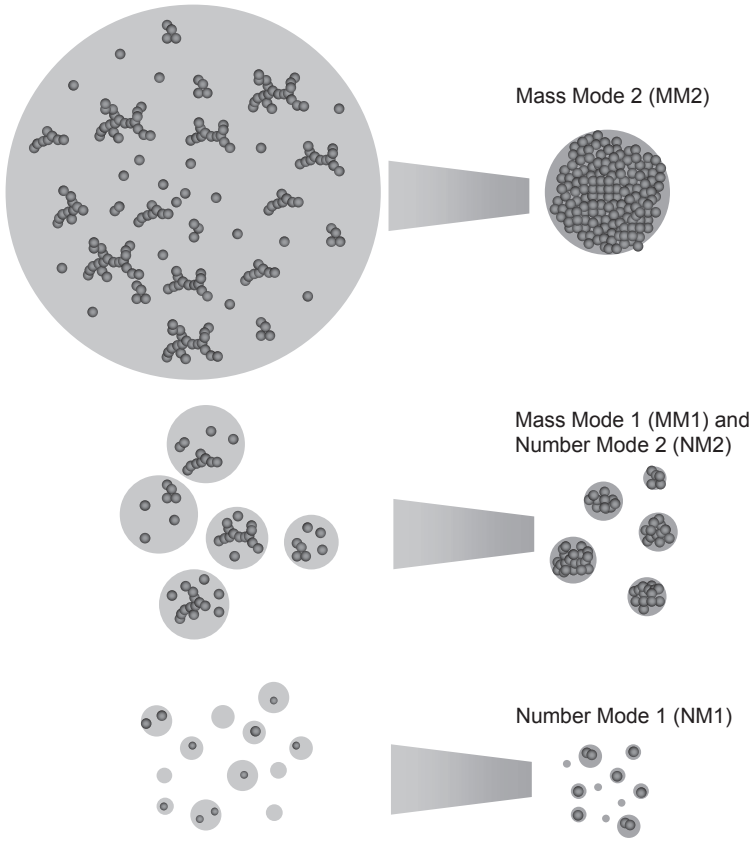

Figure 5 Diagram of potential droplet formation followed by evaporation yielding three different aerosol size modes.

previously that some HFA134a pressurized metered dose inhaler aerosols have multi-modal droplet size distributions (Smyth and Hickey 2003).

The initial droplet distribution shown in Figure 5 would lead to differences in the locations of the various modes on the particle size axis for the different suspension concentrations. The number of suspended particles in each droplet is dependant on the size of the primary particles, the concentration of those particles in suspension, and the degree of aggregation at the time of aerosolization. In the case of the DEP suspensions described above, only the concentration was known. If no aggregation is assumed, each droplet would contain a number of particles and mass of dissolved material dependant on DEP concentration. The diameter of an aerosol particle is proportional to the cubed root of its volume and, therefore, it is proportional to the cubed root of initial DEP concentration. Each particle in the aerosol from the 5.0 mg/g aerosol would have a diameter ~1.7 (cube root of 5) times larger than from the 1.0 mg/g suspension ~2.9 (cubed root of 25) times larger than from the 0.2 mg/g suspension. This phenomenon is evident in MM1 (Figure 2). As the concentration increases, the peak of that mode appears to shift to the right on the order of 1.7 and 2.9 times. This shift is not as clear for MM2 and NM1, but may be present.

If aggregation did occur to any significant extent in the propellant prior to droplet formation, an initial droplet size distribution with only one or two modes could have yielded three or more final aerosol particle size modes. In this scenario, a droplet of a particular size might or might not contain an aggregate. Those containing aggregates would have a final particle size different than those that did not, yielding two different particle size modes from one initial droplet size. This seems unlikely, however, because aggregation rates are dependant on particle concentration and differences in aggregation rates would be evident in the number particle size distributions.

Morphological characterization

SEM images of DEP can be seen in Figure 6. The particles were highly aggregated. The primary particles are not distinct, but give the powders a fluffy appearance. SEM images of DEP deposited from a 1.0 mg/g suspension on stages 3–6 of the NVCI (60 L/min) are shown in Figure 7 (particles from the other concentrations looked very similar and are not shown). The particles appear to be roughly spherical aggregates with diameters dependant on the stage on which they deposited. As with the bulk powder, the primary particles in the aggregates cannot be distinguished, but give a fluffy appearance. Images of DEP deposited from a 1.0 mg/g suspension on stage 2 of the ELPI are shown in Figure 8 (particles deposited on stages 1 and 3, and from the other concentrations looked very similar and are not shown). The particles on this stage of the ELPI (32 nm cutoff) are generally smaller and with a wider range of sizes and shapes, than those seen in the lowest stage of the NVCI (200 nm cutoff for stage 6). The physical diameters of the DEP deposited on stage 2 of the ELPI varies from <50 nm to ~1 μm, which is much larger than the aerodynamic diameter range corresponding to that stage (32–51 nm). This discrepancy may be due to the aggregation of multiple aerosol particles after deposition, but it is impossible to make that determination. It is also possible that a low density and nonspherical shape gave the particles an aerodynamic diameter much smaller than their physical diameter, although it is unlikely that a particle with a physical dimension of 1 μm had an aerodynamic diameter 20-fold less. Poor impactor efficiency and/or reintrainment of particles from the upper stages may have also contributed to the deposition of large particles on this stage.

Chemical composition

The concentration curves for B[a]P and B[k]F were linear for both wavelengths over the concentration range of 0–125 ng/ml ($R^2 > 0.99$ for all lines). The equations for these lines and average values are shown in Table 3. The combination of these equation yields two unique equations used to calculate the amount of B[a]P and B[k]F dissolved in the DCM of sonicated DEP suspensions:

$$Conc_{B[a]P} = \frac{Fl_{370} - 0.57 \cdot Conc_{B[k]F}}{1.39} \quad (1)$$

$$Conc_{B[k]F} = \frac{1.39 \cdot Fl_{395} - 0.47 \cdot Fl_{370}}{0.72} \quad (2)$$

The recovery for the known PAH concentrations from the solid phase extraction columns was 92%–98% for B[a]P and 84%–92% for B[k]F over the range of concentrations and was not dependant on concentration. The calculated PAH concentrations as functions of the DEP concentration are shown in Figure 9. This figure also shows there were no obvious differences in the amount of PAH dissolved from bulk DEP or aged or fresh DEP aerosol. The relationship appears to be linear at low concentration, as expected, but not at the highest (~1.2 mg/mL) DEP concentration. This nonlinearity was likely due to a saturation of organic compounds in the DCM at high DEP concentrations.

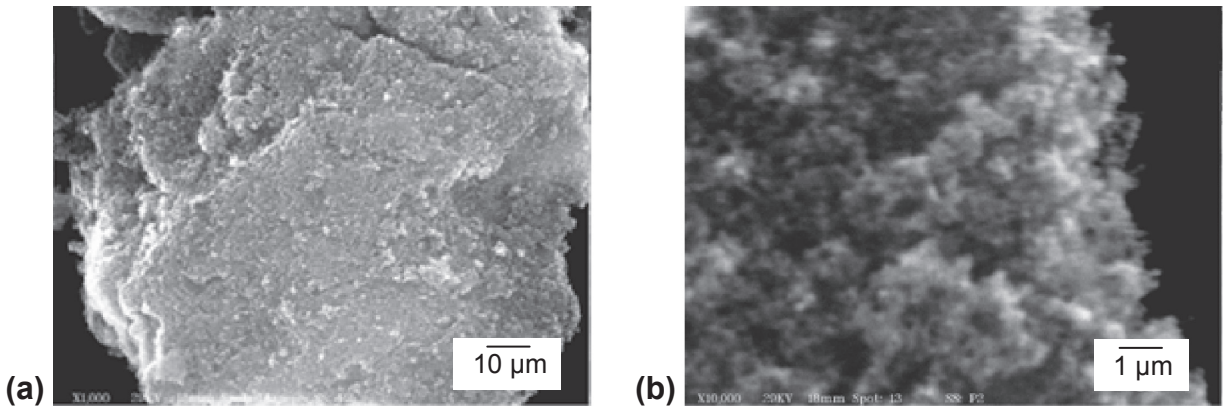

Figure 6 Scanning electron micrographs of diesel exhaust particles in bulk at (**a**) 1000X and (**b**) 10000X.

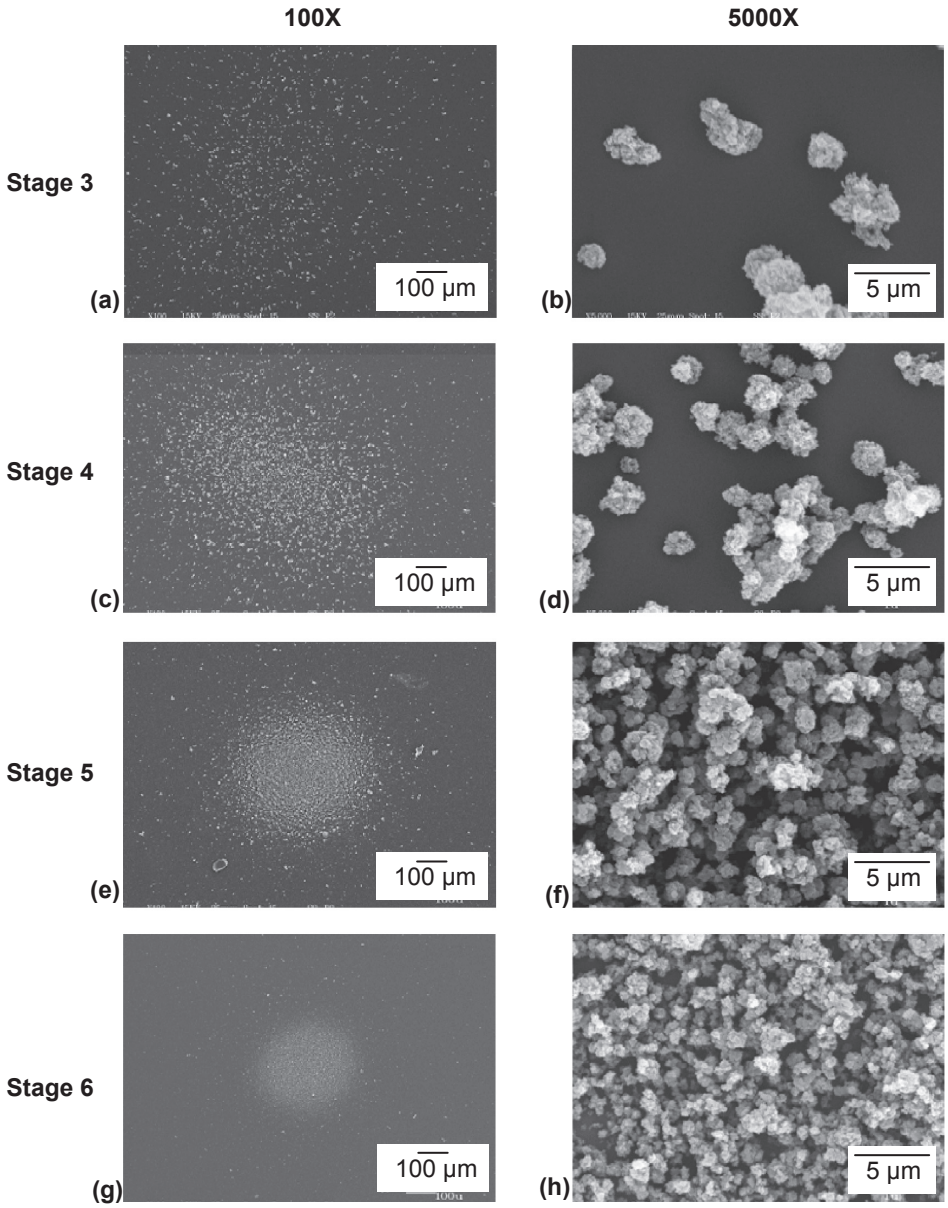

Figure 7 Scanning electron micrographs of 1.0 mg/g propellant suspension diesel exhaust particle aerosols deposited on stage 3–6 of the nonviable cascade impactor operated at 60 L/min.

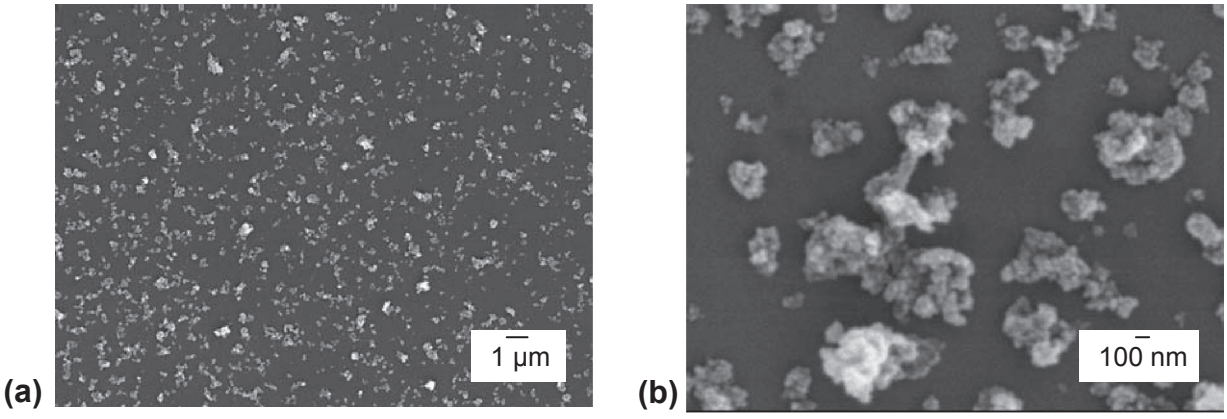

Figure 8 Scanning electron micrographs of diesel exhaust particles (DEP) deposited on a glass cover slip placed on stage 2 (32–51 nm range) of the electronic low pressure impactor following 15 actuations of a 1.0 mg/g DEP in HFA134a suspension at (**a**) 5000X and (**b**) 30000X.

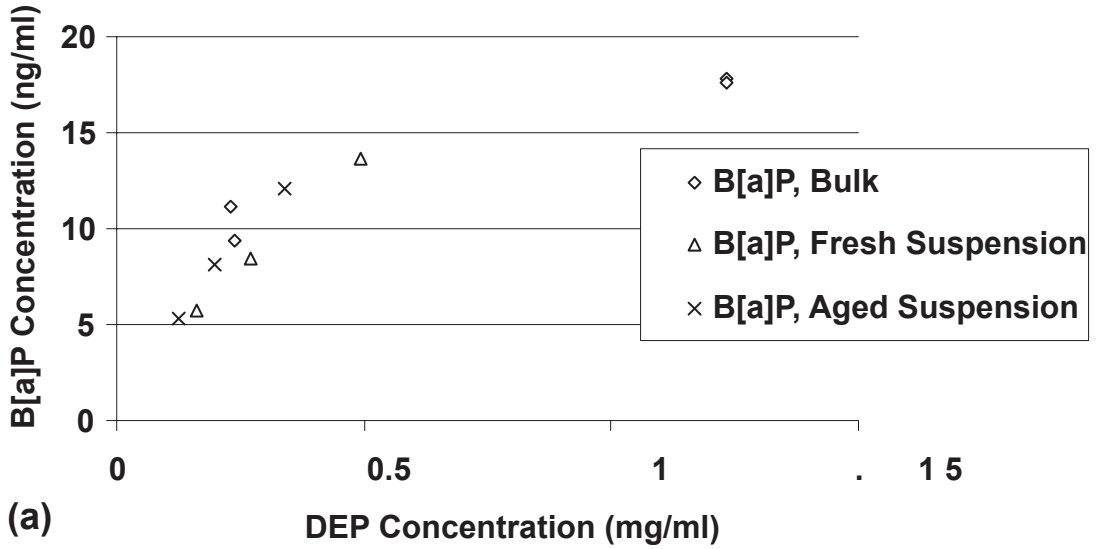

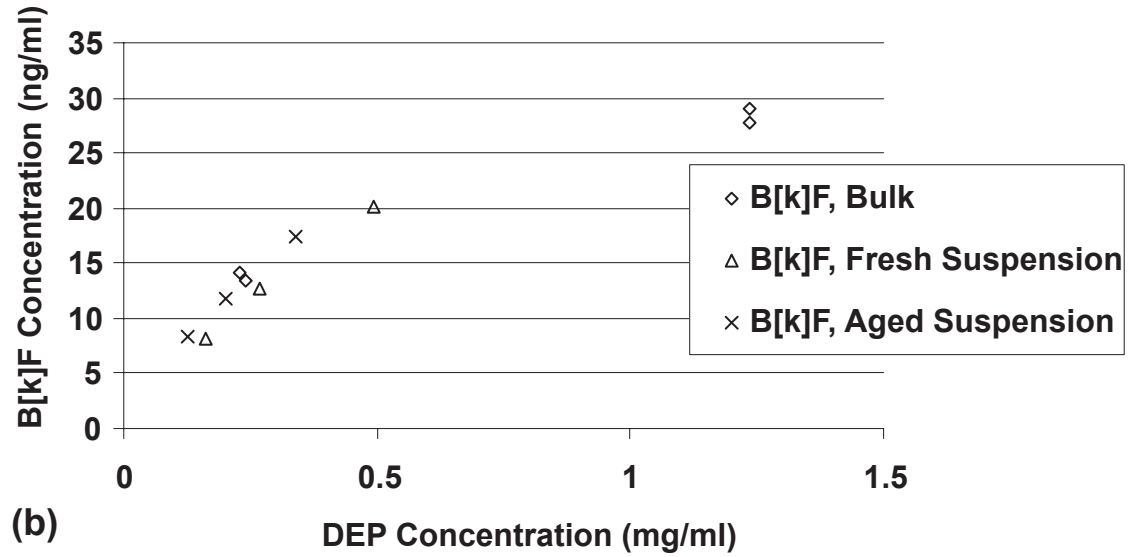

Figure 9 Concentrations of (**a**) benzo[a]pyrene (B[a]P) and (**b**) benzo[k]fluoranthene (B[k]F) as functions of the log of diesel exhaust particles (DEP) concentration calculated for bulk DEP and aerosols from 1.0 mg/g DEP suspensions that were freshly made or aged 6 months.

Table 3 Slopes of concentration curves for benzo[a]pyrene (B[a]P) and benzo[k]fluoranthene (B[k]F) fluorescence at emission wavelength of 429 nm and excitation wavelengths of 370 and 395 nm

Compound	Excitation wavelength	Run 1		Run 2		Average	
		m	b	m	b	m	b
B[a]P	370	0.69	–0.8	0.76	–1.1	0.74	–1.0
B[a]P	395	2.09	–3.9	2.24	–2.6	2.17	–3.3
B[k]F	370	1.84	–2.8	1.74	–2.4	1.79	–2.6
B[k]F	395	1.46	–2.9	1.39	–2.2	1.43	–2.6

Note: Fluorescence = Slope × Concentration (ng/ml).

Conclusions

The aim of the work described above was to generate and characterize experimental DEP aerosols relevant to atmospheric DEP for use in animal or *in vitro* toxicology studies. As stated in the introduction, DEP exist in the atmosphere in three overlapping particle size modes ranging from several nm to several μm. DEP aerosols were created by a propellant suspension method that had aerodynamic particle size distributions similar to atmospheric DEP. SEM images indicate that the aerosol particles that were generated were more highly aggregated than the fractal-like particles seen in the atmosphere. The composition of the smallest nanoparticle mode (NM1) was difficult to determine, but was probably a combination of aggregates of a small number of solid, elemental carbon particles and particles containing only compounds that dissolved from the DEP surface and remained following propellant evaporation.

The method of generating DEP aerosols by suspension in propellant could be optimized in terms of particle shape and size distribution. Altering the suspension concentration, actuator design, or propellant used could produce aerosols with different size and shape characteristics. Addition of surfactant to MDI formulations could control aggregation or physical stability of the suspensions (Vervaet and Byron 1999). Addition of chemicals of interest to the suspension could allow study of the effects of concentration of specific compounds in DEP.

The ease of use and cost benefits of generating of DEP aerosols from a bulk source as an alternative to current laboratory DEP aerosol exposure methods are apparent. There is also the potential to increase the reproducibility of exposure. There are a number of factors that influence the size and chemical concentration of DEP aerosols generated from engines in the laboratory environment including engine type, operating conditions, fuel type, and post-combustion conditions. It is difficult to tightly control all of these parameters and, thus, to ensure that a reproducible DEP aerosol is produced for inter-laboratory comparison of data. DEP aerosols generated from a standardized bulk source would be much easier to be made reproducible.

Acknowledgments

The authors are grateful to Charly King and Todd Krantz of the US EPA for diesel exhaust particle generation and collection and to Ian Gilmour, Bill Linak, and Dan Costa of the US EPA for the generous donation of diesel exhaust particles and indispensable help in the preparation of this manuscript. The authors report no conflicts of interest in this work.

References

Amakawa K, Terashima T, Matsuzaki T, et al. 2003. Suppressive effects of diesel exhaust particles on cytokine release from human and murine alveolar macrophages. *Exp Lung Res*, 29:149–64.

Atkins PJ, Crowder TM. 2004. The design and development of inhalation drug delivery systems. In: Hickey AJ (ed). Pharmaceutical inhalation aerosol technology. New York: Marcel Dekker, Inc., pp. 279–310.

Aufderheide M, Knebel JW, Ritter D. 2003. Novel approaches for studying pulmonary toxicity in vitro. *Toxicol Lett*, 140–141:205–11.

Baulig A, Garlatti M, Bonvallot V, et al. 2003. Involvement of reactive oxygen species in the metabolic pathways triggered by diesel exhaust particles in human airway epithelial cells. *Am J Physiol Lung Cell Mol Physiol*, 285:L671–9.

Bayram H, Devalia JL, Sapsford RJ, et al. 1998. The effect of diesel exhaust particles on cell function and release of inflammatory mediators from human bronchial epithelial cells in vitro. *Am J Respir Cell Mol Biol*, 18:441–8.

Bell ML, Samet JM, Dominici F. 2004. Time-series studies of particulate matter. *Annu Rev Public Health*, 25:247–80.

Bhatia R, Lopipero P, Smith AH. 1998. Diesel exhaust exposure and lung cancer. *Epidemiology*, 9:84–91.

Don Porto Carero A, Hoet PH, Verschaeve L, et al. 2001. Genotoxic effects of carbon black particles, diesel exhaust particles, and urban air particulates and their extracts on a human alveolar epithelial cell line (A549) and a human monocytic cell line (THP-1). *Environ Mol Mutagen*, 37:155–63.

Edling C, Axelson O. 1984. Risk factors of coronary heart disease among personnel in a bus company. *Int Arch Occup Environ Health*, 54:181–3.

Gamble J, Jones W, Minshall S, et al. 1987. Epidemiological-environmental study of diesel bus garage workers: chronic effects of diesel exhaust on the respiratory system. *Environ Res*, 44:6–17.

Gebhart J. 2001. Optical direct-reading techniques: Light intensity systems. In: Baron PA, Willeke K (eds). Aerosol measurement: Principles, techniques, and applications. New York: John Wiley and Sons, Inc., pp. 419–54.

Harrod KS, Jaramillo RJ, Rosenberger CL, et al. 2003. Increased susceptibility to RSV infection by exposure to inhaled diesel engine emissions. *Am J Respir Cell Mol Biol*, 28:451–63.

Henderson RF, Pickrell JA, Jones RK, et al. 1988. Response of rodents to inhaled diluted diesel exhaust: Biochemical and cytological changes in bronchoalveolar lavage fluid and in lung tissue. *Fundam Appl Toxicol*, 11:546–67.

Hinds WC. 1999. Aerosol Technology: Properties, Behavior, and Measurement of Airborne Particles. New York: John Wiley and Sons, Inc.

Hiura TS, Kaszubowski MP, Li N, et al. 1999. Chemicals in diesel exhaust particles generate reactive oxygen radicals and induce apoptosis in macrophages. *J Immunol*, 163:5582–91.

[ICRP] International Commission on Radiological Protection. 1994. Human respiratory tract model for radiological protection. ICRP Publication 66. Oxford: Elsevier.

Iwai K, Udagawa T, Yamagishi M, et al. 1986. Long-term inhalation studies of diesel exhaust on F344 SPF rats. Incidence of lung cancer and lymphoma. *Dev Toxicol Environ Sci*, 13:349–60.

Kittelson DB. 1998. Engines and nanoparticles: A review. *J Aerosol Sci*, 29(5–6):575–88.

Lewis TR, Green FH, Moorman WJ, et al. 1986. A chronic inhalation toxicity study of diesel engine emissions and coal dust, alone and combined. *Dev Toxicol Environ Sci*, 13:361–80.

Li N, Wang M, Oberley TD, et al. 2002. Comparison of the pro-oxidative and proinflammatory effects of organic diesel exhaust particle chemicals in bronchial epithelial cells and macrophages. *J Immunol*, 169:4531–41.

Lipsett M, Campleman S. 1999. Occupational exposure to diesel exhaust and lung cancer: A meta-analysis. *Am J Public Health*, 89:1009–17.

Masaki H, Susaki H, Korenaga T. 2005. Development of a micro dual beam fluorometric detector specific for microchip analysis of benzo[a]pyrene and benzo[k]fluoranthene in diesel exhaust particulate samples. *Analyst*, 130:1253–7.

Massey E, Aufderheide M, Koch W, et al. 1998. Micronucleus induction in V79 cells after direct exposure to whole cigarette smoke. *Mutagenesis*, 13:145–9.

Nemmar A, Hoet PH, Dinsdale D, et al. 2003. Diesel exhaust particles in lung acutely enhance experimental peripheral thrombosis. *Circulation*, 107:1202–8.

Nikula KJ, Snipes MB, Barr EB, et al. 1995. Comparative pulmonary toxicities and carcinogenicities of chronically inhaled diesel exhaust and carbon black in F344 rats. *Fundam Appl Toxicol*, 25:80–94.

Pope CA 3rd, Burnett RT, Thun MJ, et al. 2002. Lung cancer, cardiopulmonary mortality, and long-term exposure to fine particulate air pollution. *JAMA*, 287:1132–41.

Rudell B, Blomberg A, Helleday R, et al. 1999. Bronchoalveolar inflammation after exposure to diesel exhaust: Comparison between unfiltered and particle trap filtered exhaust. *Occup Environ Med*, 56:527–34.

Salvi S, Blomberg A, Rudell B, et al. 1999. Acute inflammatory responses in the airways and peripheral blood after short-term exposure to diesel exhaust in healthy human volunteers. *Am J Respir Crit Care Med*, 159:702–9.

Salvi SS, Nordenhall C, Blomberg A, et al. 2000. Acute exposure to diesel exhaust increases IL-8 and GRO-alpha production in healthy human airways. *Am J Respir Crit Care Med*, 161(2 Pt 1):550–7.

Sauvain JJ, Vu Duc T, Guillemin M, et al. 2003. Exposure to carcinogenic polycyclic aromatic compounds and health risk assessment for diesel-exhaust exposed workers. *Int Arch Occup Environ Health*, 76:443–55.

Smyth HD, Hickey AJ. 2003. Multimodal particle size distributions emitted from HFA-134a solution pressurized metered-dose inhalers. *AAPS Pharm Sci Tech*, 4:E38.

Takizawa H, Abe S, Okazaki H, et al. 2003. Diesel exhaust particles upregulate eotaxin gene expression in human bronchial epithelial cells via nuclear factor-kappa B-dependent pathway. *Am J Physiol Lung Cell Mol Physiol*, 284:L1055–62.

Takizawa H, Ohtoshi T, Kawasaki S, et al. 1999. Diesel exhaust particles induce NF-kappa B activation in human bronchial epithelial cells in vitro: importance in cytokine transcription. *J Immunol*, 162:4705–11.

[USEPA] US Environmental Protection Agency. 2002. Health assesment document for diesel emissions. Washington, DC: US Environmental Protection Agency.

Vervaet C, Byron PR. 1999. Drug-surfactant-propellant interactions in HFA-formulations. *Int J Pharm*, 186:13–30.

Vinegar A, Carson A, Pepelko WE, et al. 1981. Pulmonary function changes in Chinese hamsters exposed six months to diesel exhaust. *Environ Int*, 5:369–71.

Wolz L, Krause G, Scherer G, et al. 2002. In vitro genotoxicity assay of sidestream smoke using a human bronchial epithelial cell line. *Food Chem Toxicol*, 40:845–50.

Yang HM, Barger MW, Castranova V, et al. 1999. Effects of diesel exhaust particles (DEP), carbon black, and silica on macrophage responses to lipopolysaccharide: Evidence of DEP suppression of macrophage activity. *J Toxicol Environ Health A*, 58:261–78.